0026-895X/02/6101-277–284$3.00
MOLECULAR PHARMACOLOGY
Vol. 61, No. 1
1256/954954
Mol Pharmacol 61:277–284, 2002
Printed in U.S.A.

Molecular Mechanism for Endothelin-1–Induced Stress-Fiber Formation: Analysis of G Proteins Using a Mutant Endothelin$_A$ Receptor

YOSHIFUMI KAWANABE, YASUO OKAMOTO, KAZUHIKO NOZAKI, NOBUO HASHIMOTO, SOICHI MIWA, and TOMOH MASAKI,

Departments of Neurosurgery (Y.K., K.N., N.H.) and Pharmacology (Y.K., Y.O., S.M., T.M.), Kyoto University Faculty of Medicine, Kyoto, Japan

Received July 31, 2001; accepted October 11, 2001

This paper is available online at http://molpharm.aspetjournals.org

ABSTRACT

The purposes of the present study were to clarify the significance of the palmitoylation site and the cytoplasmic tail of the endothelin$_A$ receptor (ET_AR) in coupling with G proteins and to determine the subtypes of G protein that are involved in actin stress-fiber formation in Chinese hamster ovary cells that stably express ET_AR (CHO-ET_AR). For these purposes, we constructed CHO cells stably expressing an unpalmitoylated ($Cys^{383}Cys^{385–388}\rightarrow Ser^{383}Ser^{385–388}$) ET_AR (CHO-SerET_AR) and a series of truncated ET_ARs that lacked the cytoplasmic tail downstream of either of the five cysteine residues ($Cys^{383}Cys^{385–388}$). All truncated ET_ARs but not SerET_AR failed to stimulate adenylyl cyclase. With the truncated ET_ARs holding Cys^{385}, ET-1 stimulated formation of inositol phosphates, but such stimulation failed with truncated ET_ARs lacking Cys^{385}. With wild-type ET_ARs, ET-1 induced actin stress-fiber formation, which was inhibited by (*R*)-(+)-*trans*-*N*-(4-pyridyl)-4-(1-aminoethyl)-cyclohexanecarboxamide (Y-27632), a Rho-associated coiled-coil–forming protein kinase (ROCK) inhibitor. The formation was unaffected by 1-(6-{[17β-3-methoxyestra-1,3.5(10)-trien-17-yl] amino}hexyl)-1*H*-pyrrole-2,5-dione (U73122), a phospholipase C (PLC) inhibitor, or dominant negative mutants of G_{12} (G_{12}G228A) or G_{13} (G_{13}G225A), whereas it was inhibited by U73122 in combination with G_{12}G228A but not G_{13}G225A. Dibutyryl cAMP alone did not induce stress-fiber formation. With unpalmitoylated or truncated ET_ARs, the formation was sensitive to G_{12}G228A or U73122, respectively. These results indicate that 1) Cys^{385} of ET_AR is critical for coupling with G_q, 2) the cytoplasmic tail downstream of the palmitoylation sites of ET_AR is essential for coupling with G_s and G_{12}, and 3) the signal for ET-1–induced stress-fiber formation is transmitted through the G_q/PLC- and G_{12}-dependent pathway to the Rho/ROCK system.

Endothelin-1 (ET-1) has a wide variety of biological effects on various tissues and cell types (Yanagisawa et al., 1988; Masaki, 1993) that are mediated by specific heterotrimeric guanine nucleotide-binding protein (G protein)-coupled receptor subtypes, the endothelin$_A$ receptor (ET_AR) and endothelin$_B$ receptor (ET_BR) (Arai et al., 1990; Sakurai et al., 1990). The two receptors activate multiple subtypes of G proteins and can be distinguished by their selective coupling with specific G protein subtypes. When expressed in Chinese hamster ovary (CHO) cells, ET_AR couples with members of the G_q and G_s families and stimulates phospholipase C (PLC) and adenylyl cyclase. ET_BR couples with members of the G_q and G_i families, stimulates PLC, and inhibits adenylyl cyclase (Aramori and Nakanishi, 1992; Takagi et al., 1995).

ET_AR and ET_BR were shown to be palmitoylated at a cluster of cysteine residues located in the cytoplasmic tail (Horstmeyer et al., 1996; Okamoto et al., 1997). The functional role of palmitoylation and the cytoplasmic tail domain downstream of the palmitoylation site in coupling with G proteins has been studied for ET_AR and ET_BR (Horstmeyer et al., 1996; Okamoto et al., 1997). We found that in the case

This work was supported by a grant-in-aid from the Ministry of Education, Science, Sports, and Culture of Japan; by Special Coordination Funds for Science and Technology from the Science and Technology Agency; by a Research Grant for Cardiovascular Disease (11C-1) from the Ministry of Health and Welfare; and by a grant from the Smoking Research Foundation, Japan.

ABBREVIATIONS: ET-1, endothelin-1; ET_AR, endothelin$_A$ receptor; ET_BR, endothelin$_B$ receptor; CHO, Chinese hamster ovary; PLC, phospholipase C; ROCK, Rho-associated coiled-coil–forming protein kinase; CHO-ET_AR, Chinese hamster ovary cells that stably express human endothelin$_A$ receptor; CHO-$ET_AR\Delta$Cys *x*, Chinese hamster ovary cells that express human endothelin$_A$ receptor truncated at the carboxyl-terminal downstream of Cys *x* (in which *x* is 382, 383, 385, or 388); CHO-SerET_AR, Chinese hamster ovary cells that express an unpalmitoylated ($Cys^{383}Cys^{385–388}\rightarrow Ser^{383}Ser^{385–388}$) human endothelin$_A$ receptor; G_{12}G228A, dominant negative mutant of G_{12}; G_{13}G225A, dominant negative mutant of G_{13}; FCS, fetal calf serum; IP, inositol phosphate; PBS, phosphate-buffered saline; PBS-Tx, phosphate-buffered saline containing 0.1% Triton X-100; Y-27632, (*R*)-(+)-*trans*-*N*-(4-pyridyl)-4-(1-aminoethyl)-cyclohexanecarboxamide; U73122, 1-(6-{[17β-3-methoxyestra-1,3.5(10)-trien-17-yl] amino}hexyl)-1*H*-pyrrole-2,5-dione.

of ET_BR, palmitoylation is necessary for coupling with both G_q and G_i, whereas the cytoplasmic tail downstream of the palmitoylation sites is also required for coupling with G_i (Okamoto et al., 1997). On the other hand, with ET_AR, palmitoylation is reported to be essential for coupling with G_q but not with G_s, based solely on an experiment using an unpalmitoylated mutant ET_AR (Horstmeyer et al., 1996). Thus, which domain of ET_AR is necessary for coupling with G_s and which of the potential palmitoylation sites is necessary for coupling with G_q remains unknown. In this context, we first attempted to determine the structural basis essential for coupling ET_AR with G_q and G_s by focusing on several potential palmitoylation sites and the cytoplasmic tail downstream of the palmitoylation sites. For this purpose, we constructed CHO cells that stably expressed an unpalmitoylated mutant ($Cys^{383}Cys^{385–388}$→$Ser^{383}Ser^{385–388}$) ET_AR (CHO-SerET_AR) and a series of truncated ET_ARs that lacked the cytoplasmic tail downstream of any of the five cysteine residues ($Cys^{383}Cys^{385–388}$).

ET receptors were demonstrated to couple with the G_{12} subfamily, consisting of G_{12} and G_{13}, in NIH 3T3 cells (Mao et al., 1998). The G_{12} subfamily has been shown to mediate important signaling pathways such as for Rho/Rho-associated coiled-coil–forming protein kinase (ROCK)-dependent formation of actin stress fibers (Buhl et al., 1995) and vascular smooth muscle cell contraction (Gohla et al., 2000). These reports suggest that the G_{12} subfamily may play important roles in several ET-1–induced vascular disorders, such as stroke or vasospasm. Thus, the control of G_{12} subfamily activation may become a new treatment strategy for these conditions. Recently, it was shown that activation of ET_AR induces actin stress-fiber formation via G_{12} but not G_{13} (Gohla et al., 1999). However, the domains in the ET_AR that are necessary for coupling with G_{12} have not yet been elucidated. The second purpose of the present study is to reveal a functional coupling between ET_AR and G_{12}/G_{13} in CHO-ET_AR and the functional roles of the palmitoylation site and cytoplasmic tail downstream of the palmitoylation site of ET_AR in coupling of the receptor with G_{12} using mutated ET_ARs. Furthermore, the conclusion with regard to coupling of ET_AR with G_{12} is based on an experiment in which actin stress-fiber formation is lost after expression of a dominant negative mutant of G_{12} in fibroblast cell lines derived from G_q/G_{11}-double deficient mice (Gohla et al., 1999). It remains unknown whether ET-1–induced actin stress-fiber formation requires other G proteins such as G_q and G_s in addition to G_{12}. We have attempted to address this point using CHO cells expressing mutated ET_ARs. Previous reports demonstrated that CHO cells express both G_{12} and G_{13} (van de Westerlo et al., 1995; Malek et al., 2001).

Materials and Methods

Mutagenesis. The entire coding sequence of human ET_AR was subcloned into pGEM-T. The truncated ET_AR cDNAs shown in Fig. 1 were created by polymerase chain reaction. The sequence of the oligonucleotide 5′-primers for all mutants was 5′-CTCGAG-GTCGACGGTATCGATAAGCTTGATAT-3′. The sequences of the oligonucleotide 3′-primers for Δ388, Δ385, Δ383, and Δ382 were 5′-GCGGCCGCTCAACAGCAGCAGCAGAGGCAT-3′, 5′-GCGGC-CGCTCA-GCAGAGGCATGACTGGAAA-3′, 5′-GCGGCCGCTCA-GAGGCATGACTGGAAACAA-3′, and 5′-GCGGCCGCTCAT-GACTGGAAACAATTTTTA-3′, respectively. Each 3′-primer contained one nucleotide substitution to introduce a termination stop codon with a *Not*I restriction site, whereas the 5′-primer contained an *Xho*I restriction site. Fragments were amplified by the 5′-primer and each 3′-primer from ET_AR cDNA as a template. The polymerase chain reaction amplification profiles were denaturation at 94°C for 1 min, primer annealing at 55°C for 30 s, and extension at 72°C for 1 min for 30 cycles. The mutations were confirmed by sequencing, and cDNA fragments were subcloned into a *Xho*I/*Not*I restriction site of a mammalian expression vector pME18Sf predigested by *Xho*I and *Not*I.

The entire coding sequence of human ET_AR into pME18sf served as a template for unpalmitoylated mutagenesis using a QuickChange site-directed mutagenesis kit (Stratagene, La Jolla, CA). The following primers were used to substitute the cysteine residues in the cytoplasmic tail with serine residues: 5′-AATTGTTTCCAGT-CATCCCTCTCCTCCTCCTCTTACCAGTCCAAA-3′ and 5′-TTTG-GACTGGTAAGAGGAGGAGGAGAGGGATGACTGGAAACAATT-3′ to mutate $Cys^{383}Cys^{385–388}$. The mutations were confirmed by sequencing.

Wild-type G_{12} and G_{13} in pcDNA3(+) were kindly provided by Dr. Manabu Negishi (Kyoto University, Japan). G_{12}G228A and G_{13}G225A, which were shown to be the dominant negative types (Gohla et al., 1999), were generated by a QuickChange site-directed mutagenesis kit (Stratagene). Mutations were verified by sequencing.

Cell Culture and Transfection. CHO cells were maintained in Ham's F-12 medium supplemented with 10% fetal calf serum (FCS) under a humidified 5% CO_2/95% air atmosphere. For stable expression, CHO cells were transfected with expression plasmids together with pSVbsr^r using LipofectAMINE (Invitrogen, Tokyo, Japan). Cell populations expressing the bsr^r gene product were selected in Ham's F-12 supplemented with 10% FCS containing blasticidine (10 μg/ml), and clonal cell lines were isolated by colony lifting and maintained in the same medium.

^{125}I-ET-1 Binding Assay. Assays using intact cells or membrane preparations were performed exactly as described previously (Sakamoto et al., 1993).

Cyclic AMP Formation and Inositol Phosphates Formation. Cyclic AMP formation and inositol phosphate (IP) formation were determined as described previously (Okamoto et al., 1997).

Microinjection. Microinjection was performed as described previously (Okazawa et al., 1998). Briefly, cells were seeded onto glass coverslips coated with fibronectin (Iwaki Glass, Chiba, Japan), which were marked with a cross to facilitate the localization of injected cells and incubated overnight in Ham's F-12 medium containing 1% FCS. Plasmids (100 ng/μl) encoding for G_{12}G228A and G_{13}G225A were microinjected into cell nuclei. As a control, expression plasmids with-

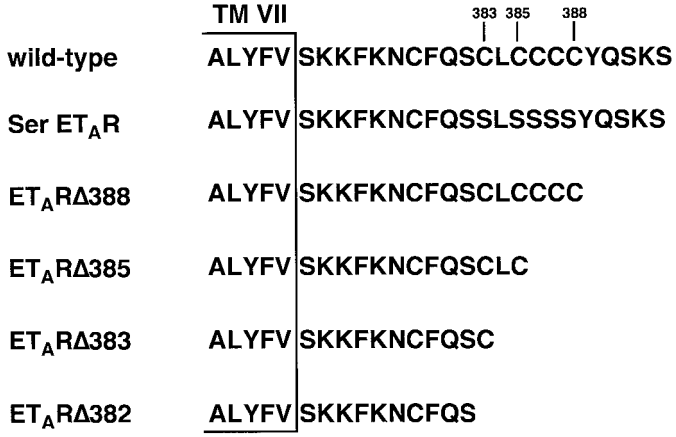

Fig. 1. Nomenclature of human ET_AR mutants. Aligned are the amino acid sequences of the carboxyl-terminal tail of the wild-type human ET_AR, unpalmitoylated mutant and four deletional mutants. The amino acid numbers of the three cysteine residues are indicated. TM VII, seventh transmembrane domain.

out inserts were microinjected in an adjacent field on the same coverslip. Microinjection was performed using a manual microinjection system (Eppendorf–5 Prime, Inc., Hamburg, Germany) equipped with an Axiovert 100 inverted microscope (Carl-Zeiss GmbH, Frankfurt, Germany).

Stress-Fiber Formation. After incubation of cells with serum-free Ham's F-12 medium for 24 h, ET-1 was added at 37°C for 5 min. Cells were washed three times with phosphate-buffered saline (PBS) and fixed with 4% paraformaldehyde in PBS at room temperature for 15 min. After being washed five times with PBS containing 0.1% Triton X-100 (PBS-Tx), the cells were incubated with fluorescein rhodamine-phalloidin (Molecular Probes, Eugene, OR) in PBS-Tx (1:200) at room temperature for 10 min. After being washed five times with PBS-Tx, the labeled cells were mounted on glass slides and examined with an MRC 1024 laser-scanning confocal microscope (Bio-Rad, Hercules, CA) equipped with an Axiovert 135 M inverted microscope (Carl-Zeiss GmbH).

Images were converted to PICT files in Adobe Photoshop (Adobe Systems Inc., San Jose, CA) and analyzed using NIH Image software (http://rsb.info.nih.gov/nih-image/) by quantifying the average pixel intensities as described previously (Barnett et al., 1997).

Drugs. Y-27632 was kindly provided by Welfide Corporation (Osaka, Japan). Chemicals were obtained from the following sources: ET-1 from the Peptide Institute (Osaka, Japan), ^{125}I-ET-1 and myo-[^{3}H]inositol from Amersham Biosciences UK, Ltd. (Little Chalfont, Buckinghamshire, UK), rhodamine-phalloidin from Molecular Probes, U73122 from Funakoshi (Tokyo, Japan), and dibutyryl cAMP from Sigma (St. Louis, MO). All other chemicals were of reagent grade and were obtained commercially.

Statistical Analysis. All results were expressed as mean ± S.E.M. The data were subjected to a two-way analysis of variance, and when a significant F value was encountered, the Newman-Keuls multiple range test was used to test for significant differences between treatment groups. A probability level of $P < 0.05$ was considered statistically significant.

Results

Stable Expression of Truncated or Unpalmitoylated Mutant ET_ARs in CHO Cells. By cotransfecting CHO cells with each expression plasmid and pSVbsr^r and then selecting for resistance against blasticidine, we obtained more than five individual clonal cell lines that stably expressed each receptor construct. In CHO cells expressing truncated mutant ET_AR, ^{125}I-ET-1 binding assays on membrane preparations from various clones gave K_d values of 30 to 120 pM and B_{max} values of 0.7 to 1.4 pmol/mg of protein. On the other hand, in CHO-SerET_AR, ^{125}I-ET-1 binding assays on membrane preparations from various clones gave K_d values of 50 to 140 pM and B_{max} values of 0.8 to 1.7 pmol/mg of protein. Cell clones showing similar levels of receptor densities were used in the subsequent study. The K_d and B_{max} values for the receptors expressed on each clone adopted are listed in Table 1.

Formation of IPs and cAMP in CHO Cells Expressing Truncated or Unpalmitoylated Mutant ET_ARs after Stimulation with ET-1. To reveal the functional significance of the palmitoylation site and the cytoplasmic tail downstream of the palmitoylation site in coupling with G_q and G_s, we tested the abilities of the mutant receptors to stimulate accumulation of [^{3}H]IPs and cAMP, respectively. [^{3}H]Palmitic acid was metabolically incorporated into CHO-ET_ARΔ388 and CHO-ET_ARΔ385 but not into CHO-ET_ARΔ383, CHO-ET_ARΔ382, or CHO-SerET_AR (data not shown).

In CHO-ET_AR, ET-1 caused a concentration-dependent stimulation of [^{3}H]IP accumulation with an EC_{50} value of 2.7 ± 0.3 nM, and the maximal effect of a ~15-fold increase was obtained at concentrations ≥10 nM (Fig. 2A). In CHO-ET_ARΔ388 or CHO-ET_ARΔ385, ET-1 caused a concentration-dependent stimulation of [^{3}H]IP accumulation with an EC_{50} value and a maximum increase that were comparable with those of CHO-ET_AR (Fig. 2A). In contrast, ET-1 failed to stimulate [^{3}H]IP accumulation in CHO-ET_ARΔ383, CHO-ET_ARΔ382, or CHO-SerET_AR (Fig. 2A).

In CHO-ET_AR, ET-1 stimulated cAMP formation with an EC_{50} of 2.7 ± 0.3 nM, and a maximal effect of an ~8-fold increase was obtained at concentrations ≥10 nM (Fig. 2B). ET-1 also stimulated cAMP accumulation in a concentration-dependent manner in CHO-SerET_AR (Fig. 2B). The EC_{50} value and the maximal effect of cAMP accumulation in CHO-SerET_AR were similar to those in CHO-ET_AR (Fig. 2B). In contrast, ET-1 failed to stimulate cAMP formation in CHO cells expressing all truncated ET_AR (Fig. 2B).

ET-1–Induced Actin Stress-Fiber Formation in CHO-ET_AR. We attempted to determine the structural basis for coupling of ET_AR with G_{12}/G_{13} and subtypes of G proteins involved in ET-1–induced stress-fiber formation. For these purposes, we examined the effects of inhibition of either one of the G protein-mediated signaling cascades by blockers and dominant negative mutants of G_{12} or G_{13} (G_{12}G228A or G_{13}G225A, respectively) on ET-1–induced actin stress-fiber formation in CHO-ET_ARΔ385, CHO-SerET_AR, and CHO-ET_AR. Subsequently, we deduced the domains of ET_AR that were critical for coupling with G_{12}, based on the structure of the mutant ET_ARs that did not have the ability to couple to G_{12}.

As reported for NIH 3T3 cells and fibroblasts (Mao et al., 1998; Gohla et al., 1999), ET-1 induced actin stress-fiber formation in CHO-ET_AR (Fig. 3B). In contrast, ET-1 failed to induce stress-fiber formation in CHO-ET_AR that had been preincubated with 10 μM Y-27632, a selective ROCK inhibitor (Fig. 3C). Stress-fiber formation was not affected by pretreatment with 5 μM U73122, a PLC inhibitor, or microinjection of G_{12}G228A or G_{13}G225A in CHO-ET_AR (Fig. 3F). This concentration (5 μM) of U73122 abolished ET-1–induced IP accumulation in CHO-ET_AR (data not shown). Notably, when the cells were subjected to microinjection of G_{12}G228A followed by pretreatment with U73122, ET-1 failed to induce stress-fiber formation (Fig. 3D). In contrast, microinjection of G_{13}G225A in combination with pretreat-

TABLE 1

Densities and affinities of wild-type and mutant ET_A receptors expressed on CHO cells

Clonal cell lines expressing each receptor construct were isolated as described under *Materials and Methods*. Binding parameters were determined by saturation isotherms of a ^{125}I-ET-1 binding assay using membrane preparations. These clones were selected because of similarities in receptor density. Deletions of amino acids in mutant receptors are shown in Fig. 1. Values are means ± S.E.M. from at least three independent experiments each done in duplicate.

Receptor Construct	K_d	B_{max}
	pM	*pmol/mg of protein*
Wild-type	52.8 ± 2.4	1.08 ± 0.16
ET_ARΔ388	65.3 ± 8.2	0.96 ± 0.05
ET_ARΔ385	49.5 ± 4.3	1.12 ± 0.08
ET_ARΔ383	39.6 ± 3.5	0.88 ± 0.10
ET_ARΔ382	56.8 ± 6.3	0.97 ± 0.12
SerET_AR	70.2 ± 4.4	1.04 ± 0.14

ment by U73122 had no effect on ET-1–induced stress-fiber formation (Fig. 3F).

To clarify the role of G_s in actin stress-fiber formation, we examined the effect of dibutyryl cAMP in quiescent CHO-ET_AR. Treatment with dibutyryl cAMP up to 10 μM alone failed to induce actin stress-fiber formation in CHO-ET_AR (Fig. 3E).

ET-1–Induced Actin Stress-Fiber Formation in CHO-SerET$_A$R and CHO-ET$_A$RΔ385. ET-1 induced stress-fiber formation in CHO-SerET_AR, in which coupling of the receptor with G_s but not G_q was retained (Fig. 4B). Like CHO-ET_AR, ET-1–induced stress-fiber formation was inhibited by preincubation of CHO-SerET_AR with Y-27632 (Fig. 4C) but was not affected by preincubation with U73122 or microinjection of G_{13}G225A (Fig. 4, E and F). Notably, unlike CHO-ET_AR, it was inhibited by microinjection of G_{12}G228A (Fig. 4D).

ET-1 induced stress-fiber formation in CHO-ET_ARΔ385, in which coupling of the receptor with G_q but not G_s was retained (Fig. 5B). Like CHO-ET_AR, ET-1–induced stress-fiber formation was inhibited by preincubation of CHO-ET_ARΔ385 with Y-27632 (Fig. 5C) but was not affected by microinjection of G_{12}G228A or G_{13}G225A (Fig. 5, E-G). Notably, unlike CHO-ET_AR, it was inhibited by preincubation with U73122 (Fig. 5D).

Discussion

^{125}I-ET-1 binding assays on intact CHO cells expressing the wild-type or truncated ET_ARs yielded K_d and B_{max} values within similar ranges (Table 1). These results were consistent with previous data (Hashido et al., 1993) and suggest that truncation of the receptor is not essential for cell surface expression and ligand binding of ET_AR. High affinity binding of ET-1 by the mutant receptors is a good indication that the overall structure of the receptor is unchanged by truncation as described earlier (Hashido et al., 1993).

As reported previously (Horstmeyer et al., 1996), with SerET_AR in which a cluster of five cysteine residues in the cytoplasmic tail as potential palmitoylation sites were substituted with serine, ET-1 failed to stimulate formation of IPs (Fig. 2A). In the present study, we extended this finding using truncated ET_ARs. The truncated ET_ARs holding Cys^{385} (CHO-ET_ARΔ385 and CHO-ET_ARΔ388) retained the ability to stimulate IP formation, whereas those lacking Cys^{385} (CHO-ET_ARΔ383 and CHO-ET_ARΔ382) lost such ability (Fig. 2A). These results taken together strongly indicate that Cys^{385} in ET_AR is critical for coupling of ET_AR with G_q and that the cytoplasmic tail downstream of the palmitoylation site is not necessary for this coupling (Fig. 6).

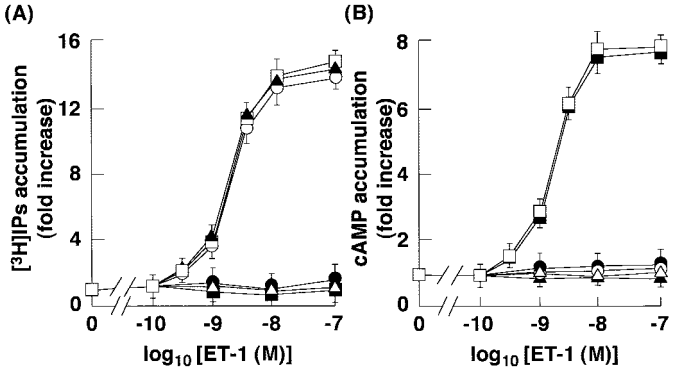

Fig. 2. Effects of ET-1 on IP (A) or cAMP (B) accumulation in CHO cells expressing wild-type or mutant ET_ARs. Formation of total IPs or cAMP after stimulation with varying concentrations of ET-1 in CHO-ET_AR (□), CHO-ET_ARΔ388 (closed triangle), CHO-ET_ARΔ385 (○), CHO-ET_ARΔ383 (△), CHO-ET_ARΔ382 (●), and CHO-SerET_AR (■). A, cells that had been incubated with *myo*-[^{3}H]inositol for 18 h were stimulated by various concentrations of ET-1 for 30 min. B, cells that were stimulated by various concentrations of ET-1 for 10 min in the presence of 3-isobutyl-1-methylxanthine. Total IPs and cAMP in the cell extract were measured as described under *Materials and Methods*. Values are expressed as -fold increases above basal values. Each data point represents mean ± S.E.M. of five experiments.

In the present study, ET-1 stimulated adenylyl cyclase in CHO-SerET_AR, which lacked potential palmitoylation sites but retained the cytoplasmic tail (Fig. 2B). These results are consistent with a previous report (Horstmeyer et al., 1996). In contrast, ET-1 failed to stimulate adenylyl cyclase in all truncated ET_ARs lacking the cytoplasmic tail, regardless of the absence or presence of palmitoylation sites of ET_AR (Fig. 2B). These results, taken together, strongly demonstrate that the cytoplasmic tail of ET_AR is critical for coupling with G_s, although it is not necessary for coupling with G_q (Fig. 6). Moreover, it was previously demonstrated that the second and third intracellular loops of ET_AR were major determinants of the selective coupling of ET_AR with G_s (Takagi et al., 1995). Therefore, we conclude that both the cytoplasmic tail and the second and third intracellular loops of ET_AR are necessary for coupling of ET_AR with G_s.

Next, we attempted to identify the subtypes of G proteins that are involved in ET-1–induced stress-fiber formation using CHO-ET_ARΔ385, CHO-SerET_AR, and CHO-ET_AR. Based on sensitivity to Y-27632, the Rho/ROCK pathway plays important roles in ET-1–induced stress-fiber formation in CHO-ET_AR (Fig. 5C) as in NIH 3T3 cells and fibroblasts (Mao et al., 1998; Gohla et al., 1999). ET-1–induced stress-fiber formation in CHO-ET_AR was affected by neither pretreatment with U73122 nor microinjection of G_{12}G228A or G_{13}G225A (Fig. 5F) but was inhibited by combined treatment with U73122 and G_{12}G228A microinjection (Fig. 3D). These results indicate that ET-1–induced stress-fiber formation is mediated via two signaling pathways (i.e., the G_q/PLC- and G_{12}-dependent pathways in CHO-ET_AR) (Fig. 6) and also that only one of the two is sufficient for actin stress-fiber formation. Moreover, the present study indicates that G_s is not involved in ET-1–induced stress-fiber formation, because dibutyryl cAMP failed to induce actin stress-fiber formation in CHO-ET_AR (Fig. 3E).

These conclusions are supported by findings obtained with SerET_AR. That is, because SerET_AR does not couple with G_q, which is one of the two signaling pathways necessary for ET-1–induced stress-fiber formation, blockade of another signaling pathway with G_{12}G228A leads to inhibition of actin stress-fiber formation. Furthermore, these results indicate that SerET_AR retains the ability to couple with G_{12}.

In CHO-ET_ARΔ385, in which coupling of the receptor with G_q but not G_s is retained, ET-1–induced stress-fiber formation was inhibited by U73122 but not G_{12}G228A. Based on the conclusion obtained from wild-type ET_AR, these data can be interpreted to mean that because ET_ARΔ385 lacks coupling with G_{12}, which is one of the two signaling pathways necessary for ET-1–induced actin stress-fiber formation, blockade of another signaling pathway with U73122 leads to inhibition of actin stress-fiber formation. Therefore, these

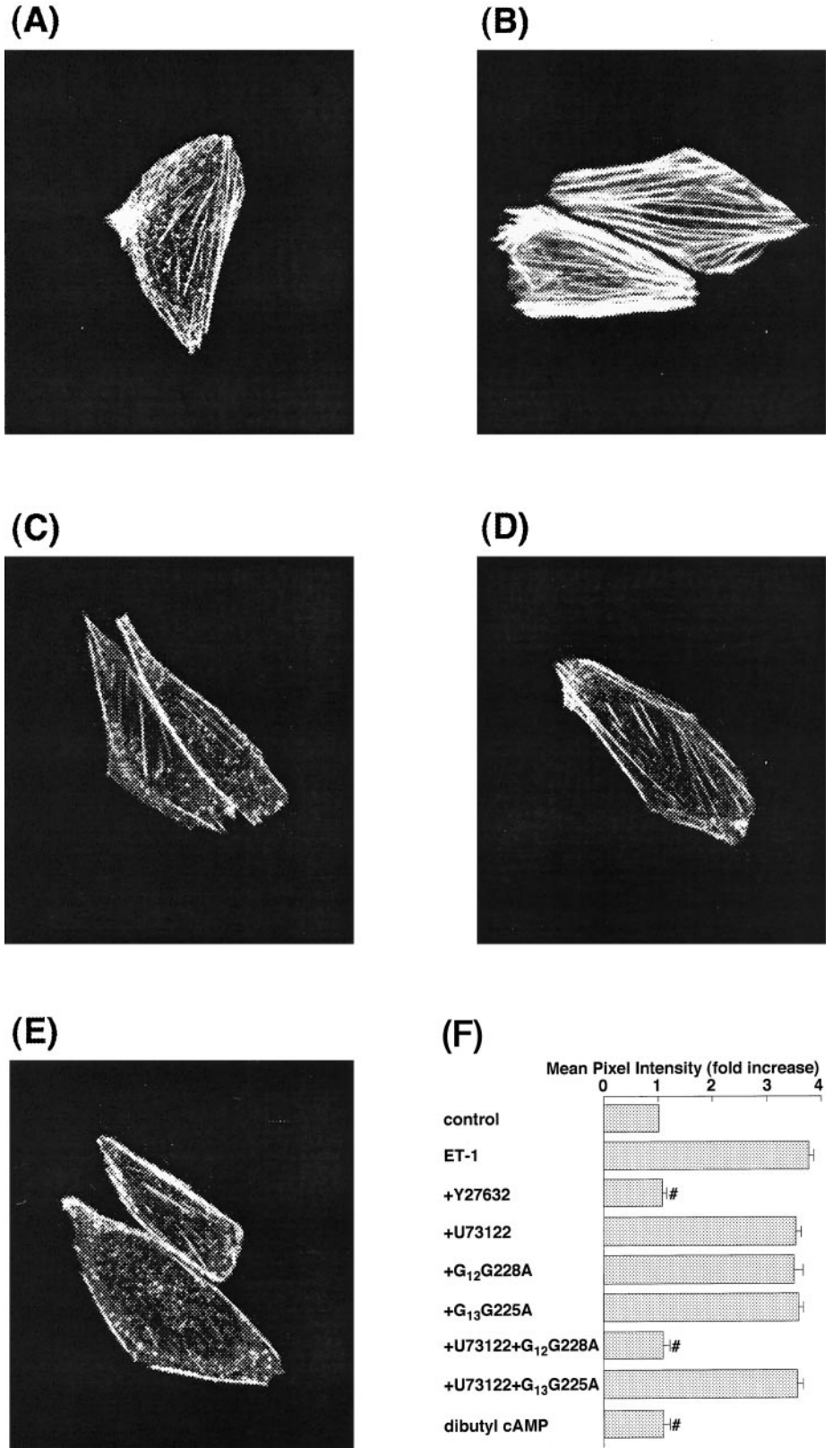

Fig. 3. A-D, effects of Y-27632, U73122, and G_{12}G228A on the ET-1–induced actin stress-fiber formation in CHO-ET_AR. Cells were stimulated with (B) or without (A) 10 nM ET-1. The effects of preincubation with 10 μM Y27632 (C) and combination treatment of G_{12}G228A microinjection and 5 μM U73122 preincubation (D) on ET-1–induced stress-fiber formation are shown. Y-27632 and U73122 were added 15 min before stimulation with ET-1. Expression plasmids encoding for G_{12}G228A and G_{13}G225A were microinjected into the cell nuclei 24 h before stimulation with ET-1. E, effects of dibutyryl cAMP on actin stress-fiber formation in CHO-ET_AR. Cells were incubated for 5 min with 10 μM dibutyryl cAMP alone. Actin stress fibers were visualized as described under *Materials and Methods*. Representative examples of stress fibers in individual cells are shown. F, pixel intensity of images was quantified using NIH Image software. Values are expressed as -fold increases above the values in the absence of ET-1. Each data point represents mean ± S.E.M. of at least 20 cells.

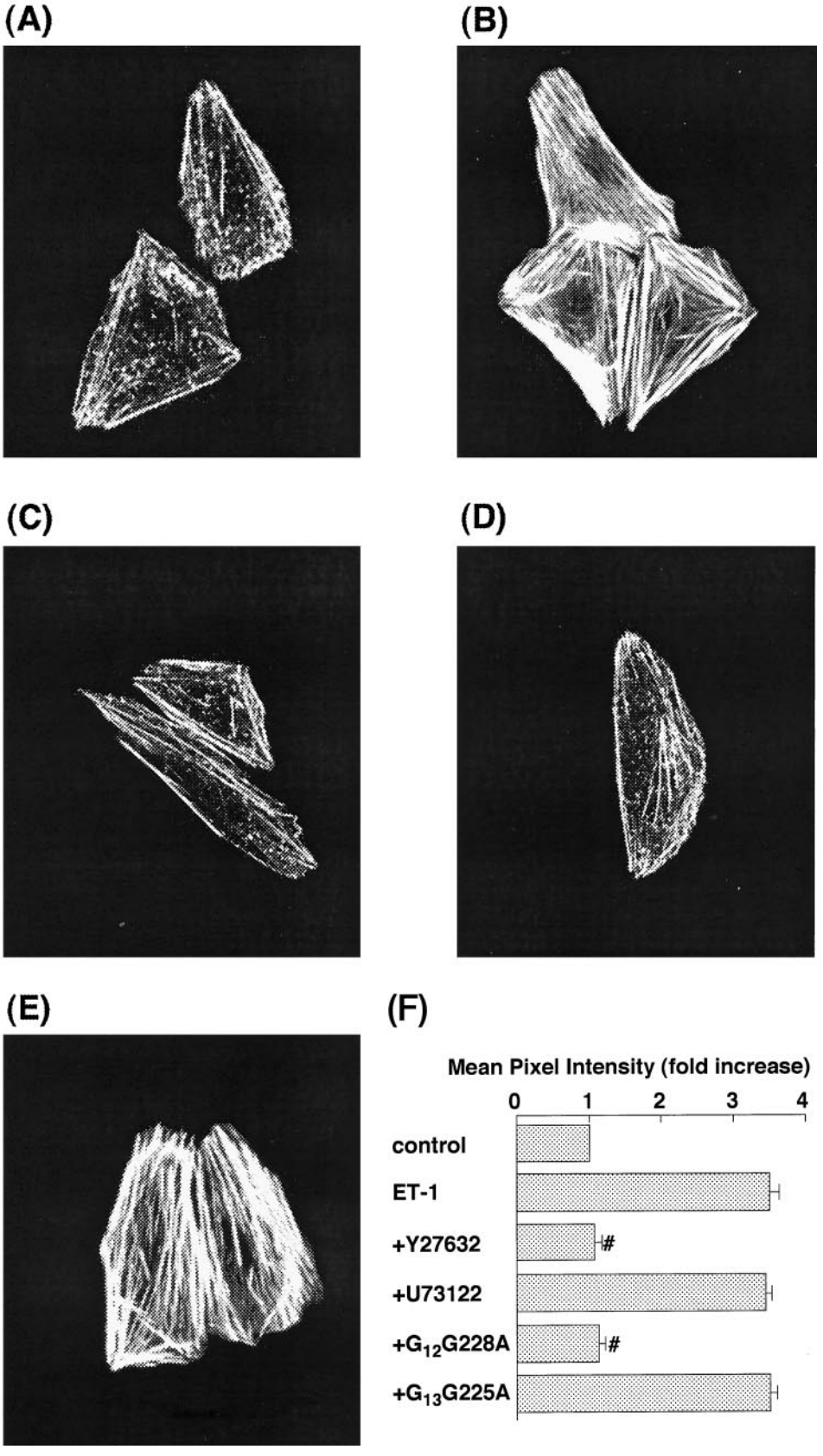

Fig. 4. Effects of Y27632, U73122, G_{12}G228A, and G_{13}G225A on ET-1–induced actin stress-fiber formation in CHO-SerET_AR. Cells were stimulated with (B) or without (A) 10 nM ET-1. C, Y-27632 at 10 μM was added 15 min before stimulation with ET-1. Expression plasmids encoding for G_{12}G228A (D) and G_{13}G225A (E) were microinjected into cell nuclei 24 h before stimulation with ET-1. Actin stress fibers were visualized as described under *Materials and Methods*. Representative examples of stress fibers in individual cells are shown. F, pixel intensity of images was quantified using NIH Image software. Values are expressed as -fold increases above the values in the absence of ET-1. Each data point represents mean ± S.E.M. of at least 20 cells.

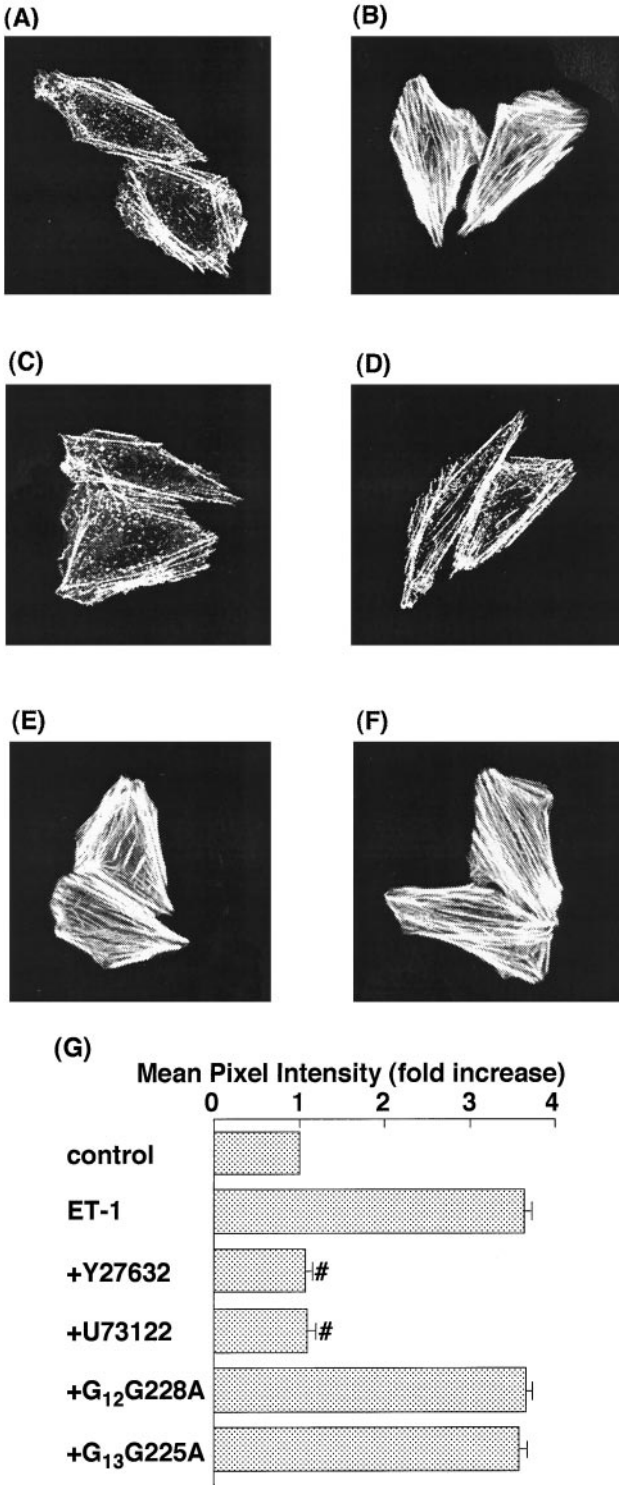

Fig. 5. Effects of Y27632, U73122, G_{12}G228A, and G_{13}G225A on ET-1–induced actin stress-fiber formation in CHO-$ET_AR\Delta385$. Cells were stimulated with (B) or without (A) 10 nM ET-1. Y-27632 at 10 μM (C) and U73122 at 5 μM (D) were added 15 min before stimulation with ET-1. Expression plasmids encoding G_{12}G228A (E) and G_{13}G225A (F) were microinjected into the cell nuclei 24 h before stimulation with ET-1. Actin stress fibers were visualized with fluorescein rhodamine-phalloidin as described under *Materials and Methods*. Representative examples of stress fibers in individual cells are shown. G, pixel intensity of images was quantified using NIH Image software. Values are expressed as -fold increases above the values in the absence of ET-1. Each data point represents mean ± S.E.M. of at least 20 cells.

results indicate that $ET_AR\Delta385$ has lost the ability to couple with G_{12}, although it can still induce stress-fiber formation via the G_q-dependent pathway.

Finally, we deduced the structural determinant for coupling of ET_AR with G_{12} based on data from experiments using mutated ET_ARs. That is, loss of coupling of $ET_AR\Delta385$ with G_{12} and retention of coupling of $SerET_AR$ with G_{12} clearly show that the cytoplasmic tail downstream of Cys^{385} but not the palmitoylation site of ET_AR is essential for coupling with G_{12}.

In conclusion, the present study showed that 1) the cytoplasmic tail downstream of the palmitoylation site of ET_AR is essential for coupling with G_s and G_{12}, 2) Cys^{385} of ET_AR is critical for coupling with G_q, and 3) the signal for ET-1–induced stress-fiber formation is mediated via the G_q/PLC- and G_{12}-dependent pathway to Rho/ROCK system in CHO-ET_AR. Thus, the presence of one of the two pathways is sufficient for stress-fiber formation.

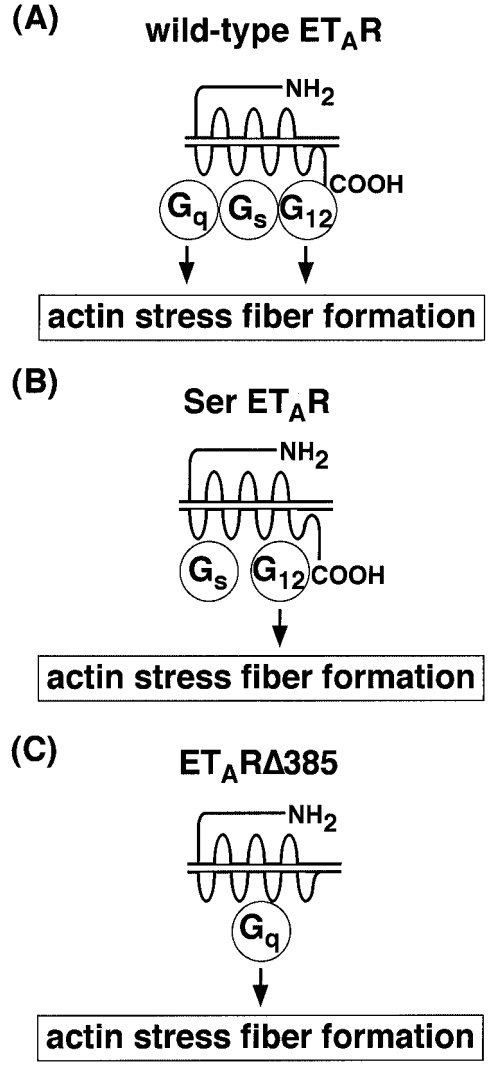

Fig. 6. Schematic representation of signaling pathways for actin stress-fiber formation activated by ET-1 in CHO-ET_AR (A), CHO-$SerET_AR$ (B), and CHO-$ET_AR\Delta385$ (C). Wild-type ET_AR couple to G_q, G_s, and G_{12}, whereas $SerET_AR$ or $ET_AR\Delta385$ couple to G_s/G_{12} or G_q, respectively. Actin stress-fiber formation is stimulated by ET-1 via G_q- and G_{12}-dependent pathways in CHO-ET_AR, whereas via G_{12}- or G_q-dependent pathway in CHO-$SerET_AR$ or CHO-$ET_AR\Delta385$, respectively. See *Results* and *Discussion* for details.

Acknowledgments

We thank Mitsubishi Pharma Corporation for the kind donation of Y-27632.

References

Arai H, Hori S, Aramori I, Ohkubo H, and Nakanishi S (1990) Cloning and expression of a cDNA encoding an endothelin receptor. *Nature (Lond)* **348:**730–732.

Aramori I and Nakanishi S (1992) Coupling of two endothelin receptor subtypes to differing signal transduction in transfected Chinese hamster ovary cells. *J Biol Chem* **267:**12468–12474.

Barnett DK, Clayton MK, Kimura J, and Bavister BD (1997) Glucose and phosphate toxicity in hamster preimplantation embryos involves disruption of cellular organization, including distribution of active mitochondria. *Mol Reprod Dev* **48:**227–237.

Buhl AM, Johnson NL, Dhanasekaran N, and Johnson GL (1995) G alpha 12 and G alpha 13 stimulate Rho-dependent stress fiber formation and focal adhesion assembly. *J Biol Chem* **270:**24631–24634.

Gohla A, Offermanns S, Wilkie TM, and Schultz G (1999) Differential involvement of Galpha12 and Galpha13 in receptor-mediated stress fiber formation. *J Biol Chem* **274:**17901–17907.

Gohla A, Schultz G, and Offermanns S (2000) Role of G12/G13 in agonist-induced vascular smooth muscle cell contraction. *Circ Res* **87:**221–227.

Hashido K, Adachi M, Gamou T, Watanabe T, Furuichi Y, and Miyamoto C (1993) Identification of specific intracellular domains of the human ETA receptor required for ligand binding and signal transduction. *Cell Mol Biol Res* **39:**3–12.

Horstmeyer A, Cramer H, Sauer T, Muller-Esterl W, and Schroeder C (1996) Palmitoylation of endothelin receptor A. Differential modulation of signal transduction activity by post-translational modification. *J Biol Chem* **271:**20811–20819.

Malek RL, Toman RE, Edsall LC, Wong S, Chiu J, Letterle CA, Van Brocklyn JR, Milstien S, Spiegel S, Lee MH. (2001) Nrg-1 belongs to the endothelial differentiation gene family of G protein-coupled sphimgosine-1-phosphate receptors. *J Biol Chem* **276:**5692–5699.

Mao J, Yuan H, Xie W, Simon MI, and Wu D (1998) Specific involvement of G proteins in regulation of serum response factor-mediated gene transcription by different receptors. *J Biol Chem* **273:**27118–27123.

Masaki T (1993) Endothelin: homeostatic and compensatory actions in the circulatory and endocrine systems. *Endocr Rev* **14:**256–268.

Okamoto Y, Ninomiya H, Tanioka M, Sakamoto A, Miwa S, and Masaki T (1997) Palmitoylation of human endothelin$_B$. *J Biol Chem* **272:**21589–21596.

Okazawa M, Shiraki T, Ninomiya H, Kobayashi S, and Masaki T (1998) Endothelin-induced apoptosis of A375 human melanoma cells. *J Biol Chem* **273:**12584–12592.

Sakamoto A, Yanagisawa M, Sawamura T, Enoki T, Ohtani T, Sakurai T, Nakao K, Toyo-oka T and Masaki T (1993) Distinct subdomains of human endothelin receptors determine their selectivity to endothelin A-selective antagonist and endothelin B-selective agonists. *J Biol Chem* **268:**8547–8553.

Sakurai T, Yanagisawa M, Takuwa Y, Miyazaki H, Kimura S, Goto K, and Masaki T (1990) Cloning of cDNA encoding a non-isopeptide-selective subtype of the endothelin receptor. *Nature (Lond)* **348:**732–735.

Takagi Y, Ninomiya H, Sakamoto A, Miwa S, and Masaki T (1995) Structural basis of G protein specificity of human endothelin receptors. A study with endothelin A/B chimeras. *J Biol Chem* **270:**10072–10078.

van de Westerlo E, Yang J, Logsdon C, and Williams JA (1995) Down-regulation of the G-proteins Gq alpha and G11 alpha by transfected human M3 muscarinic acetylcholine receptors in Chinese hamster ovary cells is independent of receptor down-regulation. *Biochem J* **310:**559–563.

Yanagisawa M, Kurihara S, Kimura S, Tomobe Y, Kobayashi M, Mitsui Y, Yazaki Y, Goto K, and Masaki T (1988) A novel potent vasoconstrictor peptide produced by vascular endothelial cells. *Nature (Lond)* **332:**411–415.

Address correspondence to: Yoshifumi Kawanabe, M.D., Department of Neurosurgery, Kyoto University Faculty of Medicine, 54 Shougoin-Kawaharachou, Sakyo-ku, Kyoto 6060-8507, Japan. E-mail: kawanabe@kuhp.kyoto-u.ac.jp